Accelerating Chan-Vese Model with Cross Modality Guided Contrast Enhancement for Liver Segmentation

Nitin Satpute[a], Juan Gómez-Luna[b], Joaquín Olivares[a]

[a]*Department of Electronic and Computer Engineering, Universidad de Córdoba, Spain*
[b]*Department of Computer Science, ETH Zurich, Switzerland*

Abstract

Accurate and fast liver segmentation remain challenging and important tasks for clinicians. Segmentation algorithms are not fast and accurate due to noise and low quality images in computed tomography (CT) abdominal scans. Chan-Vese is an active contour based powerful and flexible method for image segmentation due to better robustness for noise. But it is quite slow due to time-consuming partial differential equations, especially for large medical dataset. It can pose a problem for a real time implementation of liver segmentation and hence, an efficient parallel implementation is very important. The next and important part is the contrast of CT liver images. Liver slices are sometimes very low in contrast reducing the overall quality of liver segmentation. Hence, we implement cross modality based liver contrast enhancement as a preprocessing step to liver segmentation. GPU implementation of Chan-Vese improves average speedup by 99.811 ($\pm$ 7.65) times and 14.647 ($\pm$ 1.155) times with and without enhancement respectively in comparison to the CPU. Average dice, sensitivity and accuracy of liver segmentation are 0.656, 0.816 and 0.822 on the original liver images and 0.877, 0.964 and 0.956 on the enhanced liver images improving the overall quality of liver segmentation.

Keywords: GPU, Contrast Enhancement, Image Segmentation, Persistence, Chan-Vese

Email address: el2sasan@uco.es (Nitin Satpute)

Author's copy. How to cite: Nitin Satpute, Juan Gomez-Luna, and Joaquín Olivares. "Accelerating Chan-Vese Model with Cross-Modality Guided Contrast Enhancement for Liver Segmentation". Computers in Biology and Medicine. 124, 103930. 2020. DOI: 10.1016/J.COMPBIOMED.2020.103930

1. Introduction

Image segmentation is a popular research topic in medical imaging, as it has number of applications such as tissue detection [1], segmentation [2, 3, 4, 5], reconstruction [6], registration [6, 7] etc. There are many methods proposed for image segmentation such as region growing [8], thresholding [9], gradient approach [3], contour methods [10, 11] etc. These are either based on edge or region. They are further categorized based on histogram, spatial information of the image, convergence active contours etc [4, 12]. The active contour models are essential when the edge of the region of interest in the image is not clear and diffused [4, 13]. Computed tomography (CT) scans sometimes provide poor quality images where liver boundaries are not clearly visible and liver segmentation is essential for clinicians for the treatment of the patients.

Chan-Vese algorithm is developed on active contour models using level set approach [4, 14]. This works on the initial contours, average intensity values inside and outside the curve and try to optimize the energy based on level set approach [15, 16]. The algorithm works on the principle of energy minimization problem which relies on calculus and partial differential equation [17, 18]. It is one of the influential and effective methods in order to optimize Mumford-Shah function which includes energy terms defined in image space and contour space [12, 19, 20]. Chan-Vese is flexible and robust to segment the CT liver image which is difficult to segment using classical segmentation techniques [10, 21].

The study proposes high performance Chan-Vese model for liver segmentation by avoiding intermediate memory transfers between CPU and GPU. But the Chan-Vese model alone is not sufficient for accurate liver segmentation as it sometimes results in many false positives, lowering the sensitivity and accuracy [22, 23] degrading the quality of liver segmentation. Hence, we employ enhancement module before Chan-Vese model for segmentation. The module is based on cross modality based contrast enhancement. This works on target and guided image. We consider CT liver image as target image and MRI scan as guided image. Cross modality approach approximate the histogram of target CT scan similar to guided MR image [24, 25]. The proposed parallel approach results in fast and accurate liver

segmentation.

The contributions of the paper are as follows: We aim fast parallel Chan-Vese model for liver segmentation and apply Chan-Vese with and without liver contrast enhancement. The GPU implementation is faster compared to CPU and the liver contrast enhancement improves the quality of liver segmentation by reducing the false positives and increasing the sensitivity, dice score and accuracy of the segmentation. The average dice score, sensitivity and accuracy of the liver segmentation are 0.877 ± 0.036, 0.964 ± 0.037 and 0.956 ± 0.022 after liver contrast enhancement improving the quality of segmentation. GPU implementation of Chan-Vese segmentation algorithm improves the average speedup by 99.811 ± 7.65 times and 14.647 ± 1.155 times with and without enhancement in comparison to the CPU.

The rest of the paper is structured as follows. Section 2 briefs the background and motivation with respect to the Chan-Vese based segmentation. Section 3 explains the flow of Chan-Vese model and its parallel implementation on GPU with and without liver contrast enhancement. Performance evaluation based on quality of liver segmentation and speedup is analyzed in the Section 4. Section 5 concludes summarizing the results and main conclusions of the paper.

2. Background and Motivation

Image segmentation plays a vital role in medical image analysis. There are many methods developed for image segmentation based on edge and region [8]. Researchers have worked on active contour models for image segmentation [4, 14, 17, 18]. We explain background and motivation behind active contours and the benefits of Chan-Vese based image segmentation.

Scientists have explored snake model for segmentation. Snakes defined as a set of points around a contour [26, 27, 28]. The contour can be initialized inside the object forcing the snake to expand outside. This is Balloon Force algorithm [29, 30]. Energy of snake based model which makes a good segmentation can be defined as follows. Total energy of curve C

$$E(C) = E_{internal}(C) + E_{external}(C) \tag{1}$$

Equation 11 is a total energy where curve repeatedly evolves to minimize energy E.

$E_{internal}(C)$ and $E_{external}(C)$ depend on the shape of the snake curve and image intensities respectively.

$$E_{internal}(C) = \int_0^1 w_1||c'(s)||^2 + w_2||c''(s)||^2 ds \tag{2}$$

Equation 2 is a internal energy. Low c' means the curve is not too stretchy and it keep points on the curve together. Low c" implies the curve is not too bendy i.e. it is smooth and keeps points on curve from oscillating.

$$F(s) = -[(\frac{\partial I(X(s), Y(s))}{\partial X})^2 + (\frac{\partial I(X(s), Y(s))}{\partial Y})^2] \tag{3}$$

$$E_{external}(C) = \int_0^1 -||\nabla I(c(s))||^2 ds = \int_0^1 F(s) ds \tag{4}$$

If there is no edge then $\nabla I(c(s)) = 0$ and $F(s) = 0$ (from Equation 3 and 4). If there is a big edge then $||\nabla I(c(s))||$ is large and $F(s)$ is more negative. It implies that the $E_{external}(C)$ is lowered. The aim is to minimize E(C) from Equation 11. But the contour never sees the strong edges that are far away and snake gets hung up due to many small noises in the image [26, 27, 29, 30]. Hence researchers came up with the solution called as gradient vector flow (GVF). Instead of using image gradient, create a new vector field over image plane [31, 32]. The mathematical representation of GVF [33, 34] are given by the following equations.

$$GVF1 = [(\frac{\partial V_x}{\partial x})^2 + (\frac{\partial V_x}{\partial y})^2 + (\frac{\partial V_y}{\partial x})^2 + (\frac{\partial V_y}{\partial y})^2] \tag{5}$$

$$GVF2 = ||\nabla e||^2 ||V - \nabla e||^2 \tag{6}$$

$$cost\_GVF = \int\int \mu(GVF1) + GVF2 \ dxdy \tag{7}$$

Cost of GVF has two components defining smoothness (GVF1 from Equation 5) and edge map (GVF2 from Equation 6) as shown in Equation 7. If ∇e is big then gradient is large and V follows the edge gradient faithfully. If ∇e is small then gradient is small and V follows along to be as smooth as possible. μ is a tuning parameter to define the scaling of

smoothness in comparison to the edge map. GVF2 from Equation 6 defines the characteristic of the image based on edge where ∇e is magnitude of the edge map and $(V - \nabla e)$ shows similarity between V and ∇e. If the region has big edge (high ∇e) then $(V - \nabla e)$ should be smaller which implies V is pushed towards ∇e.

But there are problems with both snake and GVF models [26, 28, 32]. They require keeping track of number of points and point distribution. It is necessary to get points to probe into concavities. Snakes as defined can never wrap around multiple objects at once and can't do holes to get inner boundary inside region of interest. Hence researchers came up with another solution called as level sets [17, 18, 35]. Shape-intensity prior level set proposed by Wang et. al. [35] contains the atlases which are weighted in the selected training datasets by calculating the similarities between the atlases and the test image to dynamically generate a subject-specific probabilistic atlas for the test image.

The idea of level sets came from fluid dynamics in order to evolve the wavefront. Instead of parametrize the curve by a set of ordered points, discretize the image plane (x,y) and define a function f(x,y). Evolving level set function i.e. pixels where $f(x, y) = 0$ is mathematically well behaved [14, 15, 20]. Define the object contour we care about which can include multiple region of interests, inner boundary inside RoI etc. $f(x, y) > 0$ implies the pixels are inside the curve and $f(x, y) < 0$ describes the pixels outside the curve [12, 15].

In the absence of strong edges, we can use a region based formulation which is Chan-Vese model for segmentation [4, 12, 20].

$$SD_{inside} = \int_{inside} (I(x, y) - \mu_{inside})^2 dxdy \tag{8}$$

SD_{inside} from Equation 8 denotes the standard deviation of pixels inside the curve.

$$SD_{outside} = \int_{outside} (I(x, y) - \mu_{outside})^2 dxdy \tag{9}$$

$SD_{outside}$ from Equation 9 is standard deviation of pixels outside the curve.

$$SD_{total} = \lambda_1 * SD_{inside} + \lambda_2 * SD_{outside} + \lambda_3 * LC + \lambda_4 * AUC \tag{10}$$

SD_{total} from Equation 10 represents Chan-Vese algorithm where LC is length of the curve, AUC is area under the curve and $\lambda_1 > 0, \lambda_2 > 0, \lambda_3 \geq 0, \lambda_4 \geq 0$ are fixed parameters [15, 20].

The algorithm tries to maximize the difference in standard deviations of pixel distributions between inside and outside the curve.

The default value of λ is 0.1. It describes the relative weighting of curve smoothness. But after experimentation, the authors found the following values (in Equation 10) suitable for convergence and accurate liver segmentation. The weight parameter of the globe term which is inside the level set is $\lambda_1 = 0.2$. The weight parameter of the globe term which is outside the level set is $\lambda_2 = 0.2$. The weight parameter of the length term is $\lambda_3 = 0.04 * width(image) * height(image)$ and $\lambda_4 = 0.0002 * width(image) * height(image)$ is the weight parameter of the area term.

In the next section, we discuss the CPU and GPU implementation of Chan-Vese model for liver segmentation.

3. Methodology

In this section we discuss the proposed methodology based on Chan-Vese model and the impact of cross modality based contrast enhancement on liver segmentation. The sequential and parallel implementations of Chan-Vese model with and without liver contrast enhancement are explained in the following sections.

3.1. CPU Implementation of Chan-Vese

In this section, we discuss flowchart for CPU implementation of Chan-Vese model for liver segmentation. The algorithm illustrated by the flowchart in Figure 1 is based on Chan-Vese based liver segmentation used to separate liver from the other objects in CT image.

- Initialization: The aim of this step is to create a mask in order to generate a signed distance function (SDF) [14, 20]. This consists of two regions i.e. liver as foreground and non-liver region as background. The mask should be similar to liver area in order to increase the sensitivity of segmentation and reduce the time computation.

- Stopping Criteria: This step ensures the process of liver segmentation is complete or not. If the process is complete then the segmented image is stored and the process

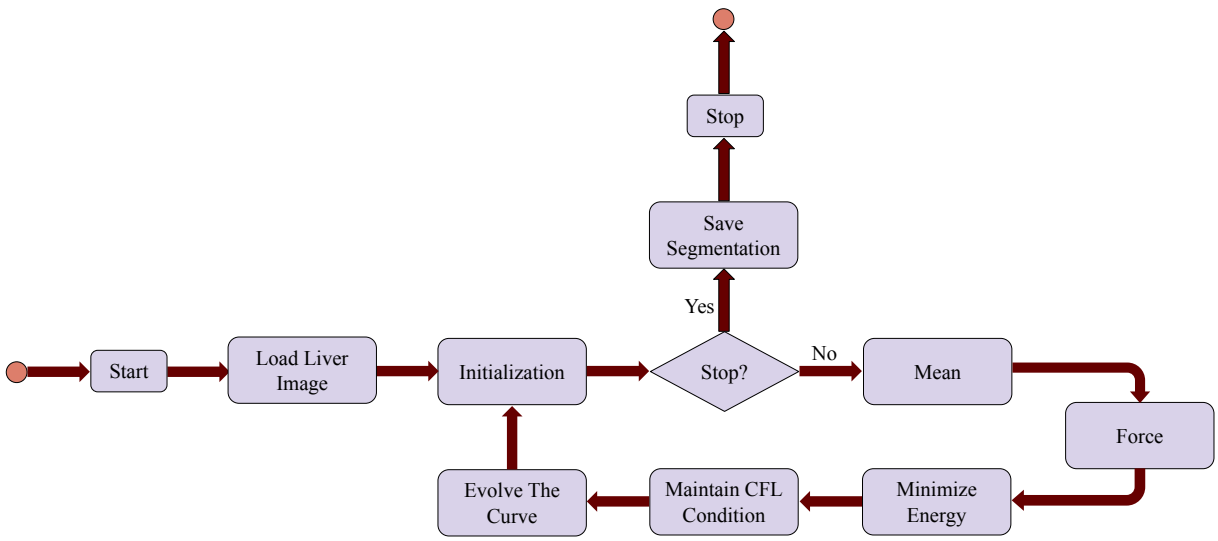

Figure 1: CPU implementation of Chan-Vese

of liver segmentation stops, else model calculates the mean of interior and exterior regions with respect to initial mask.

- Mean: This step includes computation of SDF as the first step. This is computed from the initial mask on the liver using Euclidian distance. In this work, we chose ϕ as an image with real values in order to chose distances from the curve so that distance function (SDF) is positive inside the curve and negative outside. But the computation of SDF is time consuming as it takes more time to change ϕ. Hence we apply narrow band approach to reduce the computation time by restricting the computation to a band of grid points near the level set (or mask). The SDF helps to find the average value of pixels inside and outside the curve [14, 19].

- Force: The calculation of average value of pixels inside and outside the curve are essential to compute the force from Chan-Vese energy Equation 11.

$$E = SD_{in} + SD_{out} = \int_{in} (I(x,y) - \mu_{in})^2 dxdy + \int_{out} (I(x,y) - \mu_{out})^2 dxdy \tag{11}$$

Force is computed from the image using average value of pixels inside and outside the

curve as shown in Equation 12.

$$F = \nabla E = (I(x,y) - \mu_{in})^2 + (I(x,y) - \mu_{out})^2 \tag{12}$$

Further we calculate curvature using kappa equation [12, 15] and central difference approximation scheme to approximate the derivatives of SDF with respect to x and y.

- Minimize Energy: The gradient descent algorithm helps to minimize energy given by Equation 11. The curve is updated by the calculation of SDF after small time interval and is approximated by first-order Taylor expansion.

- Maintain CFL Condition: Courant, Friedrichs, Lewy (CFL) [14, 15, 19] condition is necessary for convergence while solving the partial differential equations in order to maintain the accuracy of the curve. The equation is given as

$$C = u\Delta t/\Delta x \leq Cmax \tag{13}$$

  Where C is the courant number, u is the dependent variable which is magnitude of the velocity, Δt is the time interval and Δx is the space interval. Value of Cmax is typically 1 for the explicit methods. Equation 13 is one dimensional case of CFL condition. Courant number can be increased by increasing the time interval or decreasing the space interval. Courant number controls the stability and it is necessary to choose the space and time intervals precisely.

- Evolve The Curve: We calculate Sussman function [15] to maintain the smoothness of the curve. Re-initialization of the curve takes place and the process of Chan-Vese based segmentation continues until the liver is segmented completely and the curve can not be evolved further.

3.2. GPU Implementation of Chan-Vese

Our aim is fast parallel implementation of Chan-Vese model for liver segmentation. In this section, we discuss the GPU implementation of Chan-Vese model. Chan-Vese is an

iterative algorithm. The flow of GPU implementation of Chan-Vese for liver segmentation is shown in Figure 2.

We load the liver image and send it to the GPU memory. CPU calls Chan-Vese kernel on GPU. Each thread on GPU in parallel performs initialization of the curve. The stopping criteria is checked on the device memory to ensure the process is finished or not. If the process is finished then the control returns to the CPU storing the segmented image and the process stops, else the process of evolution of the curve continues in parallel on GPU.

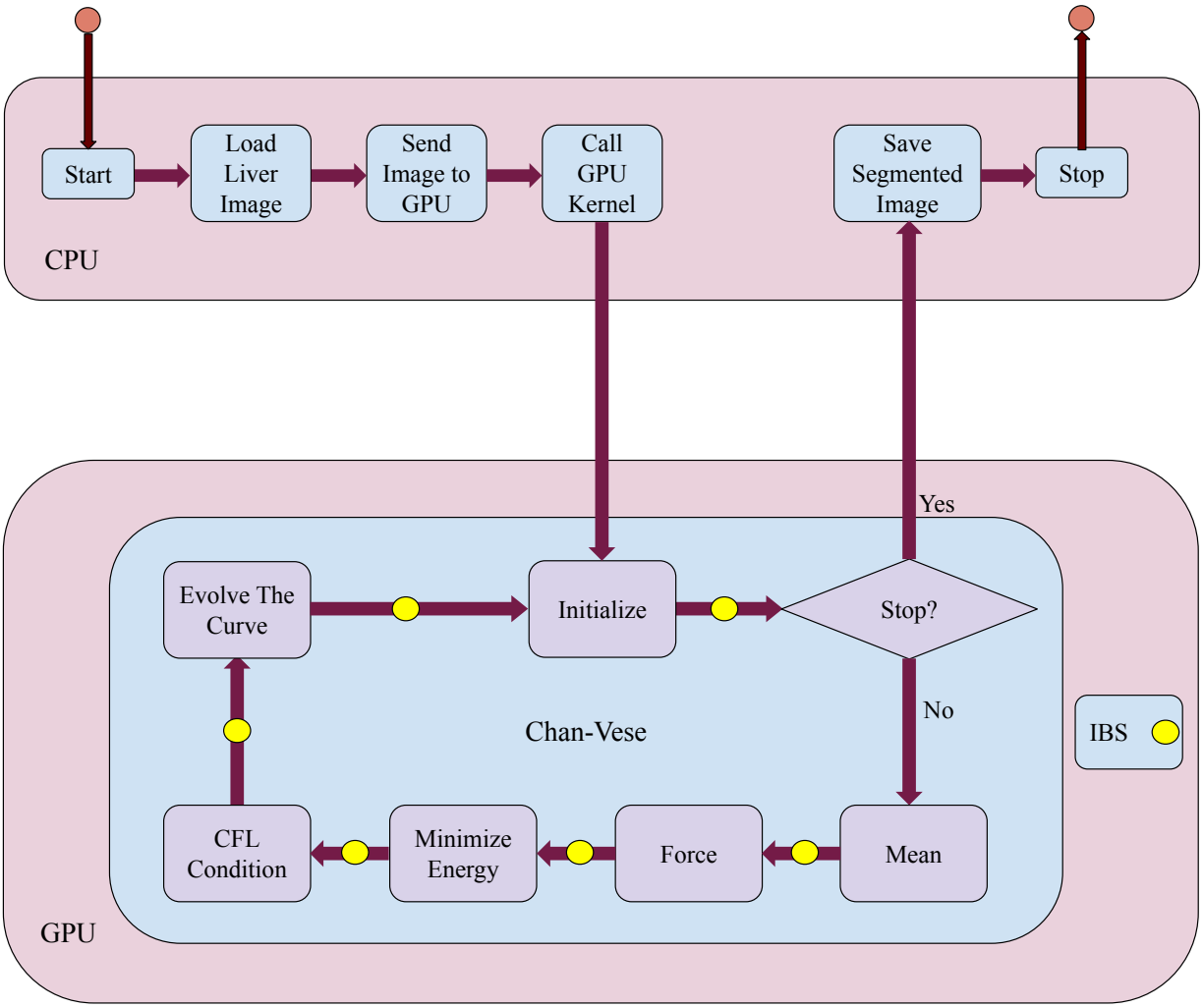

Figure 2: GPU implementation of Chan-Vese

Each thread in parallel is responsible for the calculation of average value of pixels inside

and outside of the curve. Inter block GPU synchronization (IBS) [36, 37] in between stages is essential which ensures the valid data is communicated in between the blocks. Further the Chan-Vese kernel on GPU calculates the force due to image pixels and the curvature and the gradient descent algorithm to minimize the energy given by Equation 11. All the threads maintain the CFL condition for convergence and calculate the Sussman function to maintain the smoothness of the curve. The parallel threads reinitialize the curve and the process of liver segmentation using Chan-Vese continues until the curve can not be evolved further. The process of segmentation stops and control goes back to CPU if the stopping criteria is satisfied.

These blocks communicate via IBS and the intermediate kernel calls are avoided using the proposed approach which helps in increase in the performance. The kernel invokes enough blocks of threads to compute liver segmentation. The thread blocks on the GPU are the computational units launched in parallel to perform independent operations. The maximum number of active blocks are called as persistent blocks [3, 36]. But the application may require more blocks compared to the persistent blocks. We apply grid-stride loop so that the persistent blocks are iterated to do task of remaining blocks [37, 38].

Chan-Vese is a powerful model for segmentation due to better robustness for noise but the quality of liver segmentation is questionable due to the low contrast of the liver images. Hence it is necessary to assess the impact of contrast enhancement on liver segmentation. We employ cross modality based liver contrast enhancement as pre processing step for liver segmentation. The parallel implementation of liver segmentation with contrast enhancement is discussed in the next section.

3.3. GPU Implementation of Chan-Vese with Enhancement

The Chan-Vese based liver segmentation results in false positives. In order to reduce the false positives and increase the sensitivity of liver segmentation, we enhance the CT liver image using cross modality based contrast enhancement. The flow of liver segmentation using Chan-Vese and liver contrast enhancement is provided in Figure 3.

We load CT and MR images and send it to the GPU. CPU invokes a single kernel

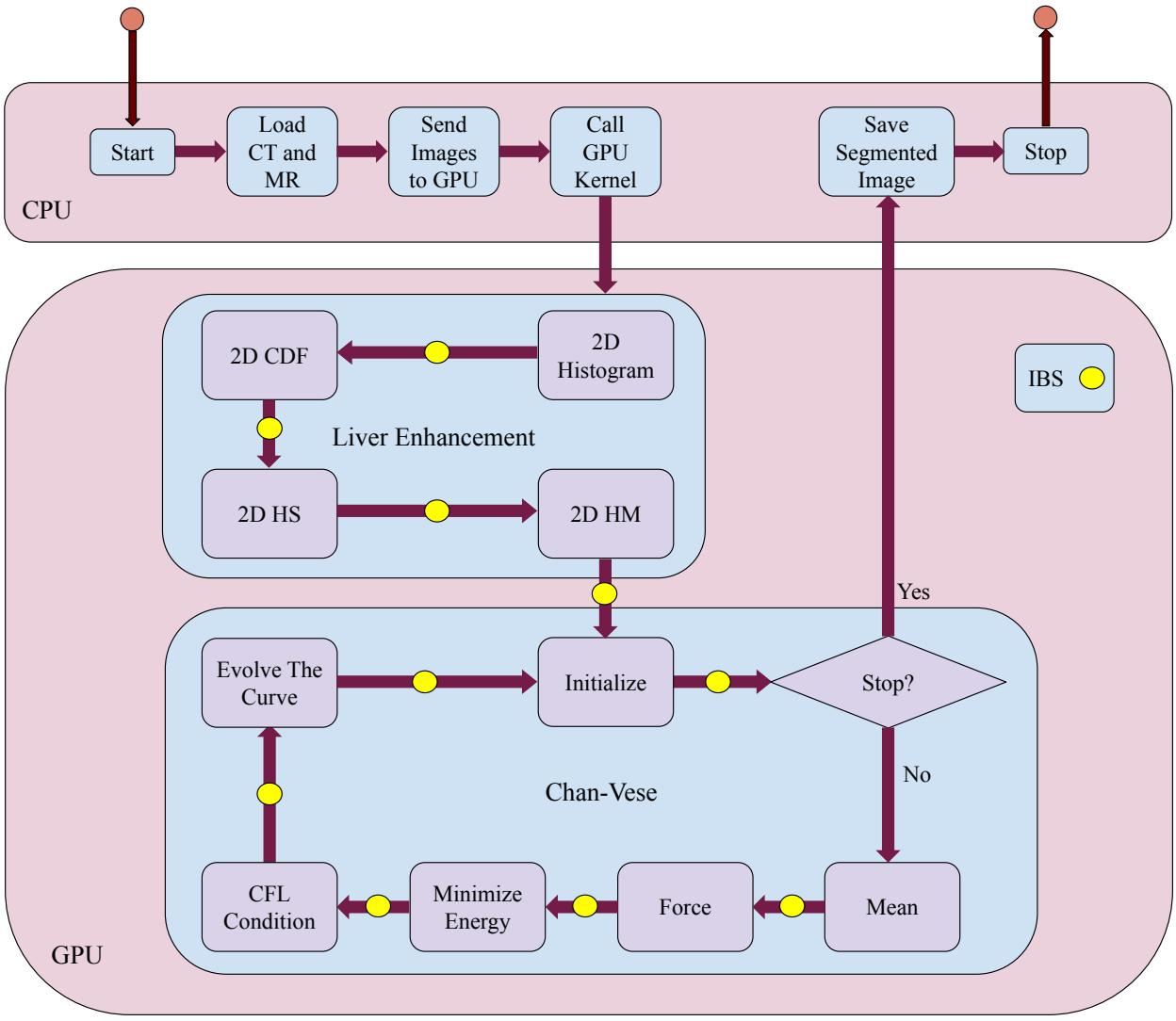

Figure 3: GPU implementation of Chan-Vese with Enhancement

for enhancement and Chan-Vese for liver segmentation. Liver enhancement improves the contrast of the CT liver image considering MR image as the guidance image. The parallel computing units on GPU matches the histogram of CT image with the guided MR image before sending it to the Chan-Vese model for segmentation. The liver contrast enhancement consists of following modules:

- 2D Histogram: The contrast enhancement module calculates the 2D histogram of both CT and MR images. A 2D histogram is a plot of a pixel and its neighbour to

discover underlying 2D frequency distribution of the image. This implies how often the neighbouring pair of values in an image occurs instead of just considering the individual pixel values [25, 39].

- 2D Cumulative Distributive Function (CDF): The 2D histograms helps to find the 2D CDFs of CT and MR images for contrast enhancement. 2D CDF calculates the probability of a possible pixel pair in CT and MR images [24, 39].

- 2D Histogram Specification (HS): This is also called as histogram equalization. HS spreads out spreads out the most frequent intensity values improving the global contrast of the image [25, 39].

- 2D Histogram Matching (HM): The process of histogram equalization onto the CT image gives the enhanced image by mapping the modified intensity values obtained from 2D histogram equalization to the corresponding pixels [24, 25].

The enhanced CT image obtained from 2D cross modality goes to the Chan-Vese model for segmentation. GPU performs the segmentation and the control returns to the CPU saving the segmented liver image. This parallel Chan-Vese model is described in the previous Section 3.2. In this next section, we discuss the performance evaluation of CP and GPU based Chan-Vese model for liver segmentation.

4. Performance Evaluation

In this section, we analyze and compare the performance of Chan-Vese model on CPU and GPU, the impact of enhancement on liver segmentation and the quality of liver segmentation using dice score, sensitivity and accuracy. We use Intel(R) Core(TM) i7-7700HQ CPU @ 2.80GHz RAM 24 GB, NVIDIA GPU GeForce GTX 1050 (RAM 4GB) and CUDA Toolkit 10.1 for the implementation and evaluate the performance of liver segmentation in the following section.

4.1. Dataset

Liver data for the research work has been acquired from The Intervention Center, University of Oslo, Norway [3, 40]. The ground truths for liver segmentation are provided by the clinician. Inter and intra observer errors exist while creating the ground truths for the input CT images. Intra observer error is when the same clinician creates the ground truth for the input CT image in different time stamps. Inter observer error is created when different clinicians create the ground truth for the same input CT image. This also depends upon the registration of input CT and MR images which are going to be used for cross modality based contrast enhancement. The errors can also be introduced if clinicians use different registration techniques for CT and MR slices. The clinicians use a 3D slicer for registration.

The CT and MRI volumes are loaded in 3D Slicer; then the ROIs (region of interests) are extracted from both volumes using 'Surface Cut' and 'Mask Volume' options available in 'Segment Editor' tool. The ROI can also be extracted using the 'Threshold' option in 'Segment Editor'. The ROIs can be registered using 'General Registration' by selecting appropriate (Degree of Freedom/ DOF) and 'Initialization Transform Mode'. Note that the registration results depend on the organs whose MRI and CT are being registered. Liver CT and MRIs are quite challenging to register.

Table 1 shows information about images of different sizes including total number of liver slices used for experimentation from a particular volume. We validate the performance on 24 liver slices obtained from 4 different registered volumes. For ground truth, images are pre-processed through locally developed applications with 3D Slicer. In some cases, the same application is used for liver segmentation and separation of portal and hepatic vessels although another possibility is to use active contour tool using ITK-SNAP and manual correction [40].

4.2. Quality of Liver Segmentation

We discuss the Chan-Vese model for liver segmentation and the impact of cross modality based contrast enhancement on liver segmentation. The segmented results using Chan-Vese

Table 1: Liver Dataset

Volume #	Total # of Slices	Image Size (wxh)	# of Slices with Liver
28059	59	462x321	6
23186	87	405x346	6
18152	139	512x512	5
10504	59	460x306	7

on original and enhanced images are shown in Figures 4, 5, and 6.

Table 2: Liver Segmentation Quality Analysis

Liver	Chan-Vese without Enhancement			Chan-Vese with Enhancement		
Slice #	Dice	Sensitivity	Accuracy	Dice	Sensitivity	Accuracy
1	0.504	0.831	0.719	0.904	0.979	0.969
2	0.533	0.669	0.748	0.895	0.961	0.966
3	0.762	0.882	0.896	0.894	0.988	0.967
4	0.759	0.868	0.890	0.879	0.991	0.961
5	0.721	0.829	0.858	0.815	0.901	0.917
Average	0.656	0.816	0.822	0.877	0.964	0.956
Std. Dev.	0.126	0.085	0.082	0.036	0.037	0.022

Figures 4a, 5a, and 6a show the liver segmentation on original CT liver slices and Figures 4b, 5b, and 6b show the liver segmentation with enhancement. We analyze Chan-Vese based segmented results from original image and enhanced image. Figures 4a2 and 4b4 show Chan-Vese based liver segmentation on the original image (Figure 4a1) and enhanced image (Figure 4b3) respectively with ground truth Figure 4a3 or 4b5. Figures 5a2 and 5b4 show liver segmentation from original image (Figure 5a1) and enhanced image (Figure 5b3) respectively with ground truth Figure 5a3 or 5b5. Similarly, Figures 6a2 and 6b4 show liver segmentation from original image (Figure 6a1) and enhanced image (Figure 6b3) respectively with ground truth Figure 6a3 or 6b5. The input CT images and ground truths

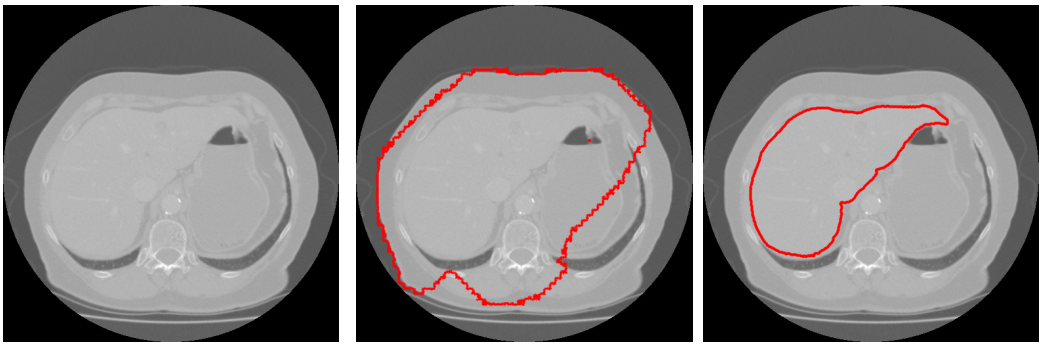

(a1) CT Image (a2) Seg (a3) GT

(a) Original Liver Image 1

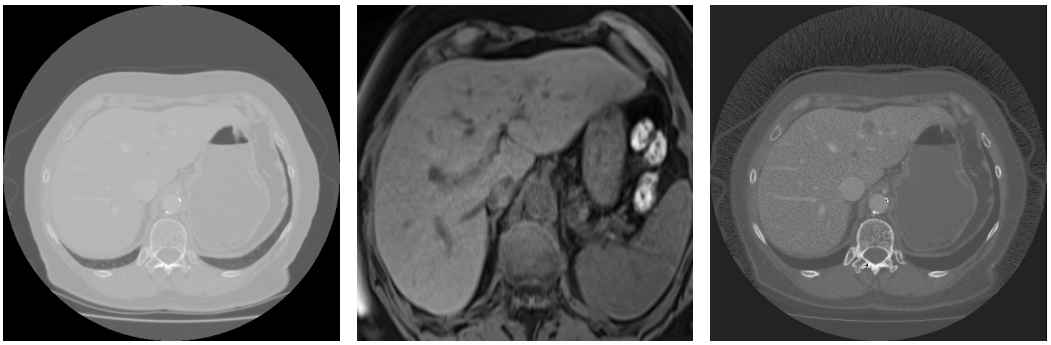

(b1) CT Image (b2) MR (b3) Enh_CT

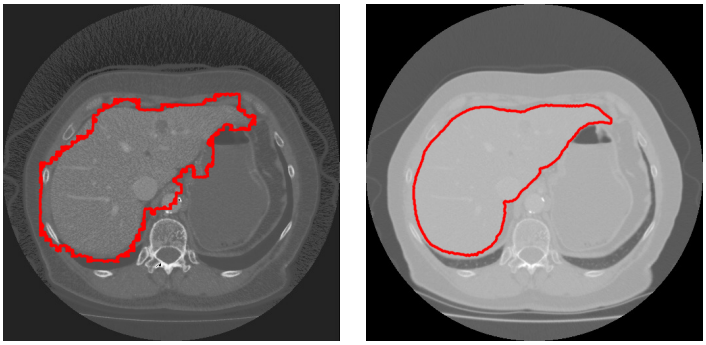

(b4) Seg (b5) GT

(b) Liver Enhancement and Segmentation from Enhanced CT Image 1

Figure 4: Liver Segmentation from Original and Enhanced CT Image 1

are same inside Figures 4, 5, and 6. For example, same input slices are shown in Figures 4a1 and 4b1, Figures 5a1 and 5b1, and Figures 6a1 and 6b1. Identical ground truth images are shown in Figures 4a3 and 4b5, Figures 5a3 and 5b5, and Figures 6a3 and 6b5. CT images (Figures 4b1, 5b1, and 6b1) and MR images (Figures 4b2, 5b2, and 6b2) are used to obtain

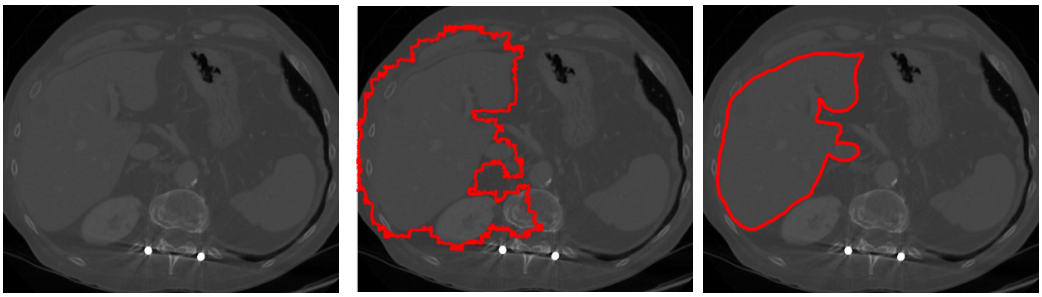

(a1) CT Image (a2) Seg (a3) GT

(a) Original Liver Image 2

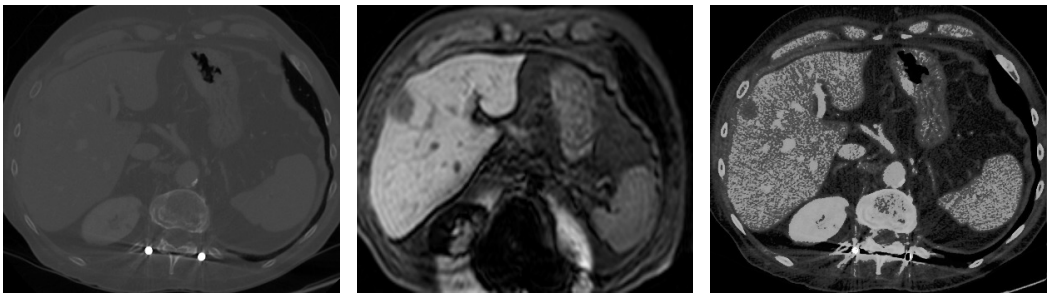

(b1) CT Image (b2) MR (b3) Enh_CT

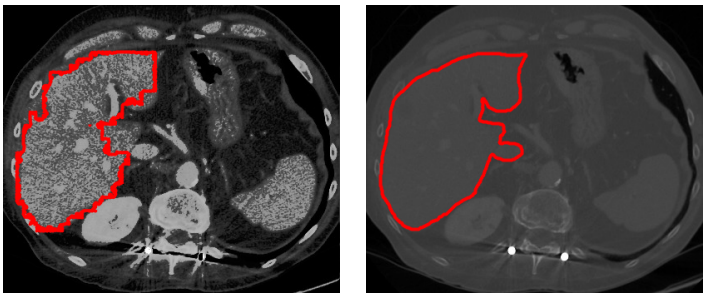

(b4) Seg (b5) GT

(b) Liver Enhancement and Segmentation from Enhanced CT Image 2

Figure 5: Liver Segmentation Original and Enhanced CT Image 2

corresponding enhanced images i.e. Figures 4b3, 5b3 and 6b3 using cross modality based liver contrast enhancement. We compare the segmented result with ground truth. It can be seen from the quality assessment of liver segmentation (Table 2) that the segmented liver is more accurate when the contrast of the liver is enhanced.

Table 2 shows the quality assessment parameters i.e. dice, sensitivity and accuracy [22, 23]. Dice measure indicates the region of overlap. Sensitivity also called as true positive rate defines whether the method is sensitive to the liver elements. Accuracy measure explains

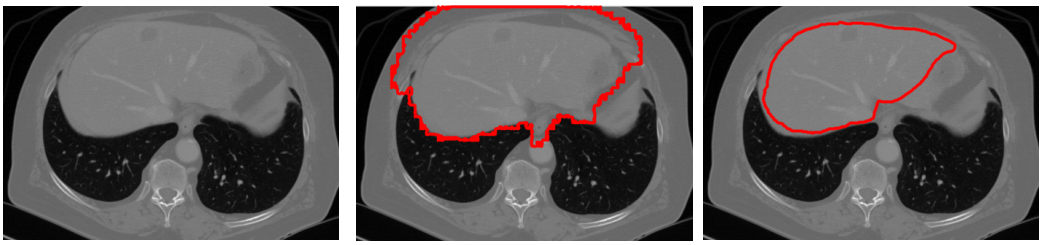

(a1) CT Image (a2) Seg (a3) GT

(a) Original Liver Image 3

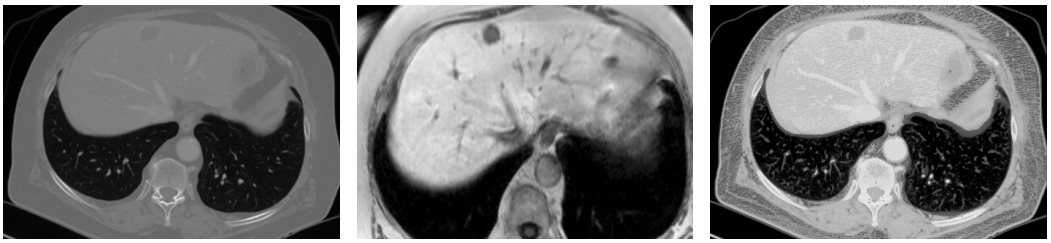

(b1) CT Image (b2) MR (b3) Enh_CT

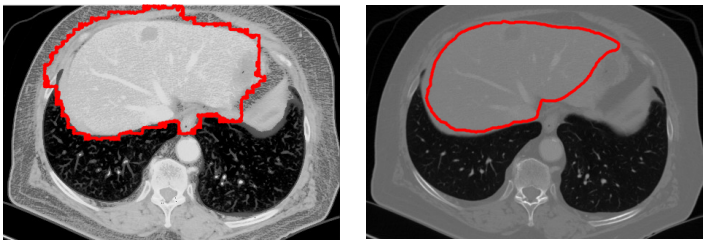

(b4) Seg (b5) GT

(b) Liver Enhancement and Segmentation from Enhanced CT Image 3

Figure 6: Liver Segmentation from Original and Enhanced CT Image 3

the number of liver and non-liver elements segmented accurately. It can be seen from the Table 2 that the average dice, sensitivity and accuracy of the liver segmentation are 0.656 $\pm$ 0.126, 0.816 $\pm$ 0.085 and 0.822 $\pm$ 0.082 on the original liver images and 0.877 $\pm$ 0.036, 0.964 $\pm$ 0.037 and 0.956 $\pm$ 0.022 on the enhanced liver images. Hence, Chan-Vese approach improves the dice, sensitivity and accuracy of liver segmentation on the enhanced liver slices.

We further analyze the performance of liver segmentation on 24 liver slices from 4 different volumes as shown in figure 7. Figures 7a, 7b, 7c and 7d show the average values of accuracy, dice score and sensitivity for Chan-Vese model with and without enhancement. It can be seen from the performance results comparison (Figures 7a, 7b, 7c and 7d) that the cross modality

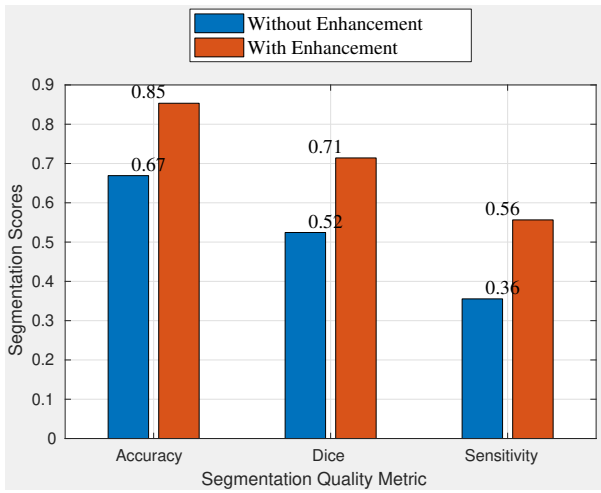

(a) Volume 28059

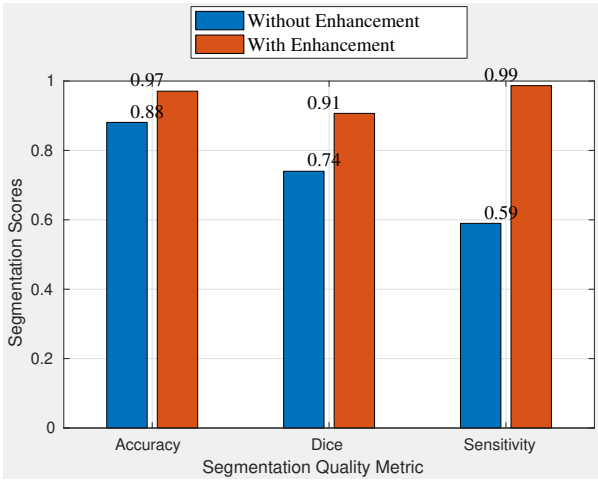

(b) Volume 23186

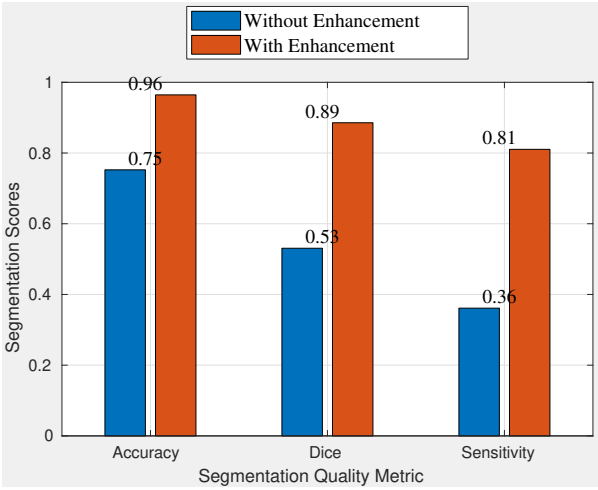

(c) Volume 18152

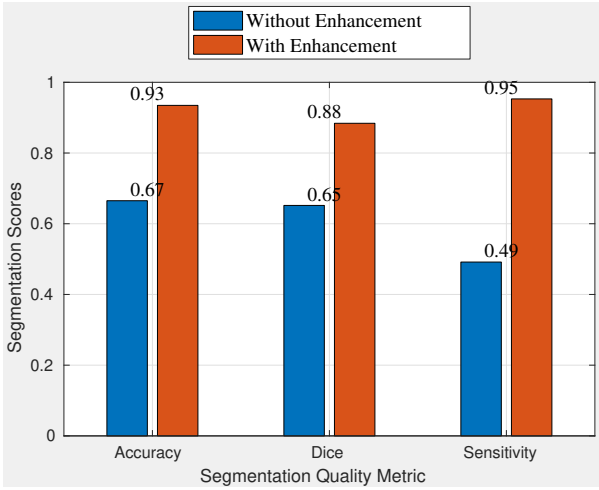

(d) Volume 10504

Figure 7: Segmentation Quality Assessment on Different Volumes

guided liver enhancement improves the quality of segmentation in terms of accuracy, dice score and sensitivity using proposed Chan Vese based liver segmentation.

There are problems with constrained B-snake model [28]. They require keeping track of the number of points and point distribution. It is necessary to get points to probe into concavities. Snakes as defined can never wrap around multiple objects at once and can't do holes to get the inner boundary inside the region of interest. The contour of points never

sees the strong edges that are far away and the snake gets hung up due to many small noises in the image. Hence the authors came up with the solution using a level set based Chan-Vese approach for liver segmentation.

Shape-intensity prior level set proposed by Wang et. al. [35] used the atlases which are weighted in the selected training datasets by calculating the similarities between the atlases and the test image to dynamically generate a subject-specific probabilistic atlas for the test image. The most likely liver region of the test image is further determined based on the generated atlas. A rough segmentation is obtained by a maximum a posteriori classification of probability map, and the final liver segmentation is produced by a shape intensity prior level set in the most likely liver region. Thus the overall process is slow due to the training phase. The process also depends upon the large datasets for training.

In the proposed work, we do not use training and hence do not need large datasets. In the absence of strong edges, region based formulation using Chan-Vese model performs well for segmentation which can be seen from performance results and the authors employ cross modality guided image enhancement as a preprocessing step which further improves the quality of segmentation. The proposed segmentation algorithm can delineate liver boundaries that have levels of variability similar to those obtained manually. The proposed approach speeds up the overall process of liver segmentation by 100 times on GPU compared to the CPU implementation.

MICCAI test data provided by the organizers of the "SLIVER07" contains clinical 3D computed tomography (CT) scans [41, 42]. The proposed approach is based on a cross modality approach where we need MR scans for the guided enhancement. We feel that it will not be fair to compare the results with Shi et. al. [41, 42] based on the dataset which does not have registered MR scans. To the best of our knowledge, this is the first non learning approach using cross modality based liver segmentation. The registered MR image is used to enhance the low quality CT image. This is done by using a non-learning approach of 2D histogram equalization and matching.

Kavur et. al. [43] reported that CT-MR liver segmentation is inferior to CT or MR image segmentation due to CT-MR visual difference. The study from CHAOS Challenge

by Kavur et. al. [43], proposes a learning based approach for segmentation taking CT-MR images as training inputs in order to increase the training data and reveal common features of incorporated modalities for an organ. The deep learning model learns from CT and MR dataset combined. The cross-modality (CT-MR) learning proved to be more challenging than individual training. Such complicated tasks could benefit from spatial priors, global topological, or shape-representations in their loss functions as employed by some of the deep learning models.

However, we show that the enhanced CT image using cross modality (CT-MR) approach provides better segmentation results in terms of dice score, accuracy and sensitivity compared to the original CT image. To the best of our knowledge, this is the first non learning approach using cross modality based liver segmentation. The registered MR image is used to enhance the low quality CT image. This is done by using a non-learning approach of 2D histogram equalization and matching. The registered CT and MR images are provided by the clinicians from Oslo University Hospital, Norway. The proposed approach is traditional. The low quality CT image is enhanced using 2D histogram matching and then Chan-Vese based level set approach is applied for accurate liver segmentation. In the next section, we discuss the speedup obtained by the proposed GPU implementation in comparison to CPU.

4.3. Speedup

In this section, we discuss the speedup obtained by GPU implementation of Chan-Vese over CPU and analyze the impact of enhancement on speedup. The speedup analysis of liver segmentation on CPU and GPU is shown in Table 3.

The computational complexity of the proposed Chan-Vese algorithm is O(N) where N is the number of elements in the CT image. So even for the large images, it is also very efficient. The average time taken by CPU implementations (with and without enhancement) are 221.302 ± 55.8 seconds and 3.49425 ± 0.752 seconds respectively and GPU implementations are 2.205 ± 0.484 seconds and 0.2345 ± 0.033 seconds respectively. Hence the GPU implementations (with and without enhancement) on NVIDIA GPU GeForce GTX 1050 with RAM 4GB provide average speedup of 99.811 ± 7.65 times and 14.647 ± 1.155 times in

Table 3: Liver Segmentation Speedup Analysis

Liver	Chan-Vese without Enhancement			Chan-Vese with Enhancement		
Slice #	CPU (s)	GPU (s)	Speedup	CPU (s)	GPU (s)	Speedup
1	4.324	0.276	15.667	276.15	2.78	99.335
2	4.117	0.256	16.082	270.098	2.44	110.696
3	2.679	0.195	13.738	173.93	1.95	89.195
4	2.857	0.211	13.54	165.03	1.65	100.018
5	3.112	0.219	14.21	175.82	1.73	101.63
Average	3.49425	0.2345	14.647	221.302	2.205	99.811
Std. Dev.	0.752	0.033	1.155	55.8	0.484	7.65

comparison to the CPU implementation on Intel(R) Core(TM) i7-7700HQ CPU @ 2.80GHz RAM 24 GB. The reason behind the obtained speedup is the avoidance of intermediate kernel calls and exploiting high level parallelism in liver contrast enhancement and Chan-Vese based liver segmentation.

Liver contrast enhancement uses 2D histogram technique which includes histogram of pair of neighbouring elements in CT and MRI image. Hence the complexity increases due to pairwise histogram analysis of cumulative distributive function and histogram matching and Chan-Vese model includes numerical calculations of partial differential equations (PDE) which are time consuming. These tasks i.e. 2D histogram calculations and PDE solutions have been implemented on NVIDIA GPU in parallel for liver segmentation providing average speedup of 99.811 ± 7.65 compared to CPU implementation. The time is computed in GPU time and it is optimized by avoiding the intermediate memory transfers.

We perform the statistical treatment of results. P value from ANOVA (analysis of variance) for the datasets is $2.43 * 10^{-14}$ which is less than 0.0005 (0.05%). We reject the null hypothesis and conclude that not all means are equal which confirms the means are statistically significant for the concerned experiments.

4.4. Discussion

Chan-Vese (CV) algorithm is sometimes quite slow due to the time-consuming computation of the partial differential equation solution, especially when dealing with the large medical images. It can pose a problem for real time applications and an efficient parallel implementation is very important. CV algorithm is a very powerful algorithm due to better robustness for noise. But there are cases when the liver segmentation is less accurate and sensitive. It is necessary to enhance the contrast of liver for more accurate liver segmentation. Hence we incorporate cross modality guided image enhancement as preprocessing step to CV for improving the quality of liver segmentation. But cross modality approach includes 2D histogram analysis which is time consuming and includes repetitive tasks of pairwise histogram analysis on liver image elements. This is also applicable to repetitive numerical calculations of PDE in CV over complete liver image. These repetitive tasks are implemented on NVIDIA GPU using thread of blocks and performance is improved significantly by exploiting parallelism over liver elements in comparison to CPU implementation.

5. Conclusion

In this paper, we propose fast parallel liver segmentation using Chan-Vese approach and study the impact of contrast enhancement on liver segmentation. The proposed approach is fast, accurate and outperforms other approaches for low quality CT liver slices. The proposed segmentation algorithm can delineate liver boundaries that have levels of variability similar to those obtained manually. GPU implementation of proposed approach speeds up the overall process of liver segmentation by 100 times compared to the CPU implementation.

Chan-Vese based liver segmentation is less sensitive (0.816 ± 0.085 from Table 2) when applied on original CT liver images. Sensitivity should be increased for more accurate liver segmentation. Hence we apply cross modality based contrast enhancement on CT liver images and segment the liver using Chan-Vese model of segmentation. The work compares CPU and GPU implementation with and without enhancement. The average dice score, sensitivity and accuracy of the liver segmentation are 0.877 ± 0.036, 0.964 ± 0.037 and

0.956 ± 0.022 on the enhanced liver images. Cross modality based contrast enhancement improves the quality of the results by decreasing the false positives and improving the dice score, sensitivity and accuracy of the segmentation. The proposed GPU implementation with enhancement improves the speedup by 99.811 ± 7.65 times over CPU implementation. Hence the parallel implementation of Chan-Vese based liver segmentation is faster when implemented on GPU and accurate when the contrast of CT liver image is enhanced.

Acknowledgements

The work is supported by the project High Performance soft tissue Navigation (HiPerNav). This project has received funding from the European Union Horizon 2020 research and innovation program under grant agreement No. 722068. We thank The Intervention Centre, Oslo University Hospital, Oslo, Norway for providing the CT images with ground truths for the clinical validation of the liver segmentation.

References

[1] M. F. Hashmi, S. Katiyar, A. G. Keskar, N. D. Bokde, Z. W. Geem, Efficient pneumonia detection in chest xray images using deep transfer learning, Diagnostics 10 (6). doi:10.3390/diagnostics10060417.

[2] K. K. Delibasis, A. Kechriniotis, I. Maglogiannis, A novel tool for segmenting 3d medical images based on generalized cylinders and active surfaces, Computer Methods and Programs in Biomedicine 111 (1) (2013) 148 – 165. doi:https://doi.org/10.1016/j.cmpb.2013.03.009.

[3] N. Satpute, R. Naseem, R. Palomar, O. Zachariadis, J. Gómez-Luna, F. A. Cheikh, J. Olivares, Fast parallel vessel segmentation, Computer Methods and Programs in Biomedicine 192 (2020) 105430. doi:https://doi.org/10.1016/j.cmpb.2020.105430.

[4] S. K. Siri, M. V. Latte, Combined endeavor of neutrosophic set and chan-vese model to extract accurate liver image from ct scan, Computer Methods and Programs in Biomedicine 151 (2017) 101–109.

[5] A. P. Rao, N. Bokde, S. Sinha, Photoacoustic imaging for management of breast cancer: A literature review and future perspectives, Applied Sciences 10 (3) (2020) 767.

[6] R. Palomar, J. Gómez-Luna, F. A. Cheikh, J. Olivares-Bueno, O. J. Elle, High-performance computation of bézier surfaces on parallel and heterogeneous platforms, International Journal of Parallel Programming 46 (6) (2018) 1035–1062.

[7] O. Zachariadis, A. Teatini, N. Satpute, J. Gómez-Luna, O. Mutlu, O. J. Elle, J. Olivares, Accelerating b-spline interpolation on gpus: Application to medical image registration, Computer Methods and Programs in Biomedicine 193 (2020) 105431. doi:https://doi.org/10.1016/j.cmpb.2020.105431.

[8] E. Smistad, T. L. Falch, M. Bozorgi, A. C. Elster, F. Lindseth, Medical image segmentation on gpus–a comprehensive review, Medical Image Analysis 20 (1) (2015) 1–18.

[9] E. Smistad, M. Bozorgi, F. Lindseth, Fast: framework for heterogeneous medical image computing and visualization, International Journal of Computer Assisted Radiology and Surgery 10 (11) (2015) 1811–1822.

[10] R. Hemalatha, T. Thamizhvani, A. J. A. Dhivya, J. E. Joseph, B. Babu, R. Chandrasekaran, Active contour based segmentation techniques for medical image analysis, Medical and Biological Image Analysis (2018) 17.

[11] X. Lu, Q. Xie, Y. Zha, D. Wang, Fully automatic liver segmentation combining multi-dimensional graph cut with shape information in 3d ct images, Scientific Reports 8 (1) (2018) 10700.

[12] X.-F. Wang, D.-S. Huang, H. Xu, An efficient local chan–vese model for image segmentation, Pattern Recognition 43 (3) (2010) 603–618.

[13] S. Tomoshige, E. Oost, A. Shimizu, H. Watanabe, S. Nawano, A conditional statistical shape model with integrated error estimation of the conditions; application to liver segmentation in non-contrast ct images, Medical Image Analysis 18 (1) (2014) 130 – 143. doi:https://doi.org/10.1016/j.media.2013.10.003.

[14] J. Duan, Z. Pan, X. Yin, W. Wei, G. Wang, Some fast projection methods based on chan-vese model for image segmentation, EURASIP Journal on Image and Video Processing 2014 (1) (2014) 7. doi:10.1186/1687-5281-2014-7.

[15] W. Aydi, N. Masmoudi, L. Kamoun, Active contour without edges vs gvf active contour for accurate pupil segmentation, International Journal of Computer Applications, Citeseer 54 (4) (2012).

[16] R. Cohen, The chan-vese algorithm, CoRR abs/1107.2782. arXiv:1107.2782.
URL `http://arxiv.org/abs/1107.2782, (2011)`

[17] A. Hoogi, C. F. Beaulieu, G. M. Cunha, E. Heba, C. B. Sirlin, S. Napel, D. L. Rubin, Adaptive local window for level set segmentation of ct and mri liver lesions, Medical Image Analysis 37 (2017) 46 – 55. doi:https://doi.org/10.1016/j.media.2017.01.002.

[18] D. Smeets, D. Loeckx, B. Stijnen, B. D. Dobbelaer, D. Vandermeulen, P. Suetens, Semi-automatic level set segmentation of liver tumors combining a spiral-scanning technique with supervised fuzzy pixel classification, Medical Image Analysis 14 (1) (2010) 13 – 20. doi:https://doi.org/10.1016/j.media.2009.09.002.

[19] L. He, S. Osher, Solving the chan-vese model by a multiphase level set algorithm based on the topological

derivative, in: International Conference on Scale Space and Variational Methods in Computer Vision, Springer, 2007, pp. 777–788.

[20] K. Zhang, H. Song, L. Zhang, Active contours driven by local image fitting energy, Pattern Recognition 43 (4) (2010) 1199–1206.

[21] E. Smistad, A. C. Elster, F. Lindseth, Gpu accelerated segmentation and centerline extraction of tubular structures from medical images, International Journal of Computer Assisted Radiology and Surgery 9 (4) (2014) 561–575.

[22] Z. Yan, X. Yang, K. Cheng, A three-stage deep learning model for accurate retinal vessel segmentation, IEEE Journal of Biomedical and Health Informatics 23 (4) (2019) 1427–1436. doi:10.1109/JBHI.2018.2872813.

[23] M. H. Yap, G. Pons, J. Martí, S. Ganau, M. Sentís, R. Zwiggelaar, A. K. Davison, R. Martí, Automated breast ultrasound lesions detection using convolutional neural networks, IEEE Journal of Biomedical and Health Informatics 22 (4) (2018) 1218–1226. doi:10.1109/JBHI.2017.2731873.

[24] T. Celik, Two-dimensional histogram equalization and contrast enhancement, Pattern Recognition 45 (10) (2012) 3810 – 3824. doi:https://doi.org/10.1016/j.patcog.2012.03.019.

[25] S.-W. Jung, Two-dimensional histogram specification using two-dimensional cumulative distribution function, Electronics Letters 50 (12) (2014) 872–874.

[26] T. Kronfeld, D. Brunner, G. Brunnett, Snake-based segmentation of teeth from virtual dental casts, Computer-Aided Design and Applications 7 (2) (2010) 221–233.

[27] S. Roy, S. Mukhopadhyay, M. K. Mishra, Enhancement of morphological snake based segmentation by imparting image attachment through scale-space continuity, Pattern Recognition 48 (7) (2015) 2254–2268.

[28] Y. Cheng, X. Hu, J. Wang, Y. Wang, S. Tamura, Accurate vessel segmentation with constrained b-snake, IEEE transactions on image processing : a publication of the IEEE Signal Processing Society 24. doi:10.1109/TIP.2015.2417683.

[29] A. Khadidos, V. Sanchez, C. Li, Active contours based on weighted gradient vector flow and balloon forces for medical image segmentation, in: 2014 IEEE International Conference on Image Processing (ICIP), 2014, pp. 902–906. doi:10.1109/ICIP.2014.7025181.

[30] Z.-B. Li, X.-Z. Xu, Y. Le, F.-Q. Xu, An improved balloon snake for hifu image-guided system, Journal of Medical Ultrasonics 41 (3) (2014) 291–300.

[31] E. Smistad, A. C. Elster, F. Lindseth, Real-time gradient vector flow on gpus using opencl, Journal of Real-Time Image Processing 10 (1) (2015) 67–74.

[32] H. Zhou, X. Li, G. Schaefer, M. E. Celebi, P. Miller, Mean shift based gradient vector flow for image segmentation, Computer Vision and Image Understanding 117 (9) (2013) 1004–1016.

[33] B. Chen, J. Zhao, E. Dong, J. Chen, Y. Zhao, Z. Yuan, An improved gvf snake model using magnetostatic theory, in: Computer, Informatics, Cybernetics and Applications, Springer, 2012, pp. 431–440.

[34] J. Zhao, B. Chen, M. Sun, W. Jia, Z. Yuan, Improved algorithm for gradient vector flow based active contour model using global and local information, The Scientific World Journal 2013.

[35] J. Wang, Y. Cheng, C. Guo, Y. Wang, S. Tamura, Shape–intensity prior level set combining probabilistic atlas and probability map constrains for automatic liver segmentation from abdominal ct images, International Journal of Computer Assisted Radiology and Surgery 11. doi:10.1007/s11548-015-1332-9.

[36] K. Gupta, J. A. Stuart, J. D. Owens, A study of persistent threads style gpu programming for gpgpu workloads, in: Innovative Parallel Computing-Foundations & Applications of GPU, Manycore, and Heterogeneous Systems (INPAR 2012), IEEE, 2012, pp. 1–14.

[37] M. Sourouri, S. B. Baden, X. Cai, Panda: A compiler framework for concurrent cpu+gpu execution of 3d stencil computations on gpu-accelerated supercomputers, International Journal of Parallel Programming 45 (3) (2017) 711–729.

[38] M. Harris, Cuda pro tip:write flexible kernels with grid-stride loops (2015).
URL `http://goo.gl/b8Vmkh`

[39] R. Naseem, F. A. Cheikh, A. Beghdadi, O. J. Elle, F. Lindseth, Cross modality guided liver image enhancement of ct using mri, in: 2019 8th European Workshop on Visual Information Processing (EUVIP), IEEE, 2019, pp. 46–51.

[40] Å. A. Fretland, V. J. Dagenborg, G. M. W. Bjørnelv, A. M. Kazaryan, R. Kristiansen, M. W. Fagerland, J. Hausken, T. I. Tønnessen, A. Abildgaard, L. Barkhatov, et al., Laparoscopic versus open resection for colorectal liver metastases, Annals of surgery 267 (2) (2018) 199–207.

[41] C. Shi, Y. Cheng, F. Liu, Y. Wang, J. Bai, S. Tamura, A hierarchical local region-based sparse shape composition for liver segmentation in ct scans, Pattern Recognition 50 (2016) 88–106.

[42] C. Shi, Y. Cheng, J. Wang, Y. Wang, K. Mori, S. Tamura, Low-rank and sparse decomposition based shape model and probabilistic atlas for automatic pathological organ segmentation, Medical image analysis 38 (2017) 30–49.

[43] A. E. Kavur, N. S. Gezer, M. Barış, P.-H. Conze, V. Groza, D. D. Pham, S. Chatterjee, P. Ernst, S. Özkan, B. Baydar, et al., Chaos challenge–combined (ct-mr) healthy abdominal organ segmentation, arXiv preprint arXiv:2001.06535.